PROSPECTS
IN PHARMACEUTICAL SCIENCES

Prospects in Pharmaceutical Sciences, 23(4), 220-234
https://prospects.wum.edu.pl/

Original Article

DEVELOPMENT AND OPTIMIZATION OF DANAZOL CO-CRYSTAL LOADED TABLET TO TREAT ENDOMETRIOSIS

Vidya Patil*[1], Shivraj Jadhav[1], Sunil Mahajan[2]

[1]*Department of Pharmaceutics, Divine College of Pharmacy, Nashik, Maharashtra, India 422301.*

[2]*Department of Pharmaceutical Chemistry, Divine College of Pharmacy, Nashik, Maharashtra, India 422301.*

** Correspondence, e-mail: vidyapatil03112001@gmail.com*

Received: 25.05.2025 / Revised: 21.07.2025 / Accepted: 06.08.2025 / Published first online: 01.10.2025 / Published in final version: 31.12.2025

ABSTRACT

Objectives: To develop, optimize, and characterize danazol co-crystal-loaded tablets for enhanced solubility and dissolution in order to improve therapeutic efficacy in endometriosis treatment. Methods: Danazol co-crystals were prepared using various co-formers through a solvent evaporation technique and characterized by FTIR, DSC, and XRD. Co-crystals were formulated into tablets using direct compression and optimized through a 3^2 factorial design, varying sodium croscarmellose (8—24 mg) and PVP K-30 (4—20 mg) concentrations. Formulations were evaluated for pre-compression properties, physical parameters, disintegration, dissolution, and stability. Results: Danazol-malonic acid co-crystals (1:2 ratio) exhibited the highest solubility enhancement (11.42 ± 0.53 µg/mL, 13.76-fold increase). XRD confirmed the formation of a new crystalline phase with distinct peaks at 19° and 21° 2θ. The quadratic models for both disintegration time (R^2 = 0.9971) and drug release (R^2 = 0.9483) demonstrated excellent predictive capability. Formulation VF7 (24 mg sodium croscarmellose, 4 mg PVP K-30) was identified as optimal with rapid disintegration (74.0 ± 3.2 seconds) and superior dissolution (83.6 ± 3.4% at 30 minutes, 95.8 ± 2.0% at 60 minutes) compared to the marketed product (75.2 ± 2.7% at 60 minutes). The optimized formulation maintained stability under accelerated conditions (40°C/75% RH) for three months. Conclusion: The optimized danazol co-crystal tablet formulation successfully overcame the solubility and dissolution limitations of this poorly soluble drug, potentially enhancing bioavailability and therapeutic efficacy while reducing dosing frequency for endometriosis patients. This approach presents a promising platform for improving clinical outcomes and patient compliance in endometriosis management.

KEYWORDS: danazol, co-crystallization, solubility enhancement, factorial design, endometriosis.

1. Introduction

Endometriosis affects approximately 10% of reproductive-aged women globally, affecting an estimated 190 million individuals worldwide [1]. This chronic inflammatory condition, characterized by the growth of endometrial tissue outside the uterine cavity, imposes a substantial economic burden of $69—119 billion annually in the United States alone through direct healthcare costs and lost productivity [2]. Current pharmaceutical interventions primarily consist of hormonal therapies and analgesics that provide symptomatic relief rather than disease modification, with up to 50% of patients experiencing treatment failure or intolerable side effects [3]. The disease significantly diminishes quality of life, with 38% of patients reporting reduced work productivity and 11% experiencing complete work disability [2]. Despite recent advances in minimally invasive surgical techniques, recurrence rates remain high at 40—50% within five years post-operation [4]. The persistent challenges in effectively managing endometriosis highlight the urgent need for novel therapeutic approaches with improved efficacy and tolerability profiles [5].

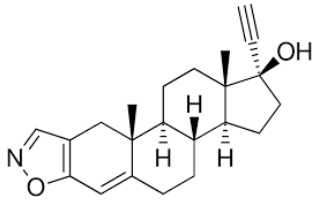

Fig. 1. Chemical structure of danazol.

Danazol, a synthetic androgen derivative (17α-ethinyl testosterone) (Fig. 1), represents a potentially valuable therapeutic agent for endometriosis due to its multimodal mechanism of action [6,7]. The compound exhibits a molecular weight of 337.46 g/mol and demonstrates moderate lipophilicity (log P = 4.53), aqueous solubility values ranging from 0.4—0.6 µg/mL under standard conditions, with variations up to 10—18 µg/mL depending on experimental conditions, temperature, and analytical methods employed. Structurally characterized by a modified steroid nucleus with an ethynyl group at C-17 and a 2,3-isoxazole ring, danazol exerts its therapeutic effects through inhibition of pituitary gonadotropin secretion, direct suppression of endometrial tissue growth, and modulation of inflammatory pathways [8]. Clinical studies have demonstrated efficacy rates of 60—90% for pain reduction and endometriotic lesion regression. However, conventional danazol formulations require high doses (400—800 mg daily) to achieve therapeutic plasma concentrations, often resulting in androgenic side effects that limit patient compliance and clinical utility [9]. Recent investigations into structural modifications and alternative delivery systems present promising opportunities to revitalize this established compound for improved endometriosis management [10].

The co-crystallization approach represents an innovative strategy to overcome the pharmaceutical limitations of danazol through the formation of supramolecular structures with complementary co-formers [11]. This technology exploits non-covalent interactions, predominantly hydrogen bonding, π-π stacking, and van der Waals forces, to create crystalline lattices with enhanced physicochemical properties [12]. Co-crystallization of danazol with selected GRAS (Generally Recognized as Safe) compounds has demonstrated substantial improvements in aqueous solubility (up to 12-fold increase) and dissolution rates (5-fold enhancement) in preliminary investigations [13]. The tablet delivery system incorporating these co-crystals employs modified release technology to optimize pharmacokinetic parameters and reduce dosing frequency. Recent advances in pharmaceutical engineering have demonstrated various approaches for co-crystal formation and formulation, with solvent evaporation techniques showing particular promise for laboratory-scale development and characterization studies. This approach potentially addresses multiple challenges simultaneously: improving bioavailability, reducing required doses, minimizing side effects, and enhancing patient adherence for endometriosis management [14].

The present study aims to develop, characterize, and optimize danazol co-crystal loaded tablets specifically designed for endometriosis treatment. The research will evaluate various co-formers for optimal physicochemical enhancement, establish robust manufacturing processes, and assess in vitro performance parameters to demonstrate therapeutic advantages over conventional formulations.

2. Materials and Methods

2.1. Materials

Danazol (USP grade, 99.5% purity) was obtained from Sciquaint Innovations (Pune, India). Malonic acid, oxalic acid, fumaric acid, and caprylic acid (all analytical grade) were purchased from Sciquaint Chemicals (Pune, India). Microcrystalline cellulose (Avicel PH-102) and sodium croscarmellose (AcDiSol) were procured from FMC Neeta Chemicals (Pune, India). Polyvinylpyrrolidone K-30, Magnesium stearate, and phosphate buffer pH 6.8 were obtained from Research Lab Fine Chem Industries (Mumbai, India). Danocrine® tablets (200 mg danazol, Sanofi-Aventis, France, Batch No. DAN2023-045, Exp. Date: 12/2025) were procured from a licensed pharmacy (Pune, India). All other chemicals and reagents used were of analytical grade and used as received without further purification.

2.2. Methods

2.2.1. Preparation of Calibration Curve

Calibration curve of danazol was prepared in methanol:phosphate buffer pH 6.8 (7:3). By dissolving 100 mg danazol in 100 mL of the solvent mixture, a stock solution (1000 µg/mL) was prepared. Appropriate dilutions of the stock solution were carried out to prepare working standard solutions (5—30 µg/mL). The absorbance at 286 nm was determined using a UV-visible spectrophotometer (Shimadzu UV-1800, Japan). The absorbance vs. concentration calibration curve was drawn, and the linear regression equation was determined. The values of coefficient of determination (R^2), slope, and y-intercept were calculated. The limit of detection (LOD) and limit of quantification (LOQ) were determined based on the standard deviation of the response and the slope of the calibration curve using the ICH Q2(R1) guidelines. LOD was calculated as $3.3 \times \sigma/S$ and LOQ as $10 \times \sigma/S$, where σ is the standard deviation of the y-intercept and S is the slope of the calibration curve [15].

2.2.2. FTIR Analysis

FTIR spectroscopy was employed to assess molecular interactions between danazol and co-formers (malonic acid, oxalic acid, fumaric acid, caprylic acid) in physical mixtures prior to co-crystallization. Approximately 2—3 mg of each sample was placed directly onto the diamond crystal and compressed. Spectra were obtained in the range of 4000—400 cm^{-1} with a resolution of 4 cm^{-1} and 24 scans per spectrum. Characteristic peaks were identified and compared across samples to understand structural changes and intermolecular interactions. Regions near functional groups engaged in hydrogen bonding (carbonyl, hydroxyl, and amine groups) were given special attention [16].

2.2.3. Differential Scanning Calorimetry (DSC) Analysis

Thermal behavior of pure components and physical mixtures was characterized using differential scanning calorimetry (DSC 214 Polyma, NETZSCH). Samples (3—5 mg) were accurately weighed and sealed in aluminum pans with pierced lids. An empty aluminum pan was used as a reference. Samples were heated from 30°C to 300°C at a heating rate of 10°C/min under a nitrogen purge (50 mL/min). The onset temperature, peak temperature, and enthalpy of fusion were recorded. Co-crystal formation was confirmed by comparing thermal profiles of co-crystals with those of pure components and physical mixtures, with particular focus on melting point depression, appearance of new thermal events,

and disappearance of endotherms associated with pure components [17,18].

2.2.4. Formulation of Co-crystals by Solvent Evaporation

Co-crystals of danazol with various co-formers were prepared using the solvent evaporation technique. Danazol was combined with selected co-formers (malonic acid, oxalic acid, fumaric acid, and caprylic acid; analytical grade, Sciquaint Chemicals, India) in 1:1 and 1:2 ratios. Each mixture was dissolved in 10 mL ethanol (99.9%) in a glass beaker at room temperature (25 ± 2°C) [19]. Solutions were stirred at 100 rpm for 30 minutes and left undisturbed for 24—72 hours until complete solvent evaporation. The resulting crystals were collected, dried in a desiccator for 24 hours, passed through a #60 mesh sieve, and stored in airtight containers. All preparations were performed in triplicate (n=3) [18].

2.2.5. Solubility Determination of Danazol Co-crystals

The shake flask method was used to determine aqueous solubility. Each sample was weighted in excess of 50 mg, added to 10 mL distilled water in glass vials, and agitated in an orbital shaker (Thermo Scientific MaxQ 4000) at 37 ± 0.5°C and 100 rpm for 48 hours. The suspensions were passed through 0.45 µm membrane filters (Millipore, India). Dilutions of the filtrates were done accordingly, and the concentration of danazol was determined at λmax of 286 nm with a nanomolar concentration range on a UV-visible spectrophotometer (Shimadzu UV 1800, Japan). Calibration curves (R^2 > 0.999) were constructed using danazol standards (1—50 µg/mL) made in the same medium. All measurements were performed in triplicate (n=3), [20,21].

2.2.6. Experimental Design for Tablet Formulation

A 3^2 full factorial design was employed with two independent variables: X_1 (sodium croscarmellose concentration, 8—24 mg/tablet) and X_2 (PVP K-30 concentration, 4—20 mg/tablet), each at three levels (-1, 0, +1) as shown in Table 1. Nine formulations were prepared according to the design matrix generated using Design-Expert® software (version 13.0, Stat-Ease Inc., USA). The dependent variables were Y_1 (disintegration time) and Y_2 (% drug release at 30 minutes).

Table 1. Variables in 3^2 Factorial Design for Danazol Co-crystal Tablets.

Independent Variables			
Variables	Quantity (mg/tablet)		
	Low (-1)	Medium (0)	High (+1)
X_1: Sodium croscarmellose	8.0	16.0	24.0
X_2: PVP K-30	4.0	12.0	20.0
Dependent Variables			**Goal**
Y_1: Disintegration Time (seconds)			Minimize
Y_2: Drug Release at 30 min (%)			Maximize

The mathematical relationship was established using the following equation [22,23]:

$$Y = b_0 + b_1X_1 + b_2X_2 + b_{12}X_1X_2 + b_{11}X_1^2 + b_{22}X_2^2 \ldots\ldots(1)$$

ANOVA was performed to validate the model ($p<0.05$ considered significant), and response surface plots were generated to visualize the effects of variables on responses.

2.2.7. Preparation of Danazol Co-crystal Tablets

Co-crystallization product containing danazol (200 mg equiv.) was prepared by direct compression into danazol tablets. The danazol co-crystal formulation was blended with microcrystalline cellulose (diluent), sodium croscarmellose (superdisintegrant), PVP K-30 (binder), and colloidal silicon dioxide (2.0 mg, 0.5% w/w) for 15 minutes using a laboratory blender. Magnesium stearate (2.0 mg, 0.5% w/w) was then added and mixed for additional 3 minutes to ensure uniform distribution without over-mixing. Subsequently, the powder blends were compressed using a rotary tablet press (Rimek Mini Press-II) at a compression force of 10 to 12 kN using 10 mm standard concave punches. Therefore, tablet weight was kept in the range of 400 ± 20 mg [24,25]. Detail formulation of batches is gven in Table 2.

Table 2. Formulation Composition of Danazol Co-crystal Tablets (mg/tablet).

Ingredients (mg/tablet)	VF1	VF2	VF3	VF4	VF5	VF6	VF7	VF8	VF9
Danazol: Malonic Acid Co-crystal (1:2)	323	323	323	323	323	323	323	323	323
Sodium Croscarmellose	8.0	8.0	8.0	16.0	16.0	16.0	24.0	24.0	24.0
PVP K-30	4.0	12	20	4	12	20	4	12	20
Microcrystalline Cellulose	60.67	52.67	44.67	52.67	44.67	36.67	44.67	36.67	28.67
Colloidal Silicon Dioxide	2.0	2.0	2.0	2.0	2.0	2.0	2.0	2.0	2.0
Magnesium Stearate	2.0	2.0	2.0	2.0	2.0	2.0	2.0	2.0	2.0
Total Weight (mg)	400	400	400	400	400	400	400	400	400

Danazol: Malonic Acid Co-crystal (1:2) contains equivalent of 200 mg Danazol.

2.2.8. Pre-compression Evaluation of Danazol Co-crystal Powder Blends

2.2.8.1 Angle of Repose

The fixed funnel method was used to determine the angle of repose. A glass funnel with its tip at a fixed height (h = 2 cm) above a flat surface covered with graph paper was mounted with a 10 mm orifice in the funnel. For the next trial, 10 g powder blend was carefully poured through the funnel until the apex of the conical pile reached the lower tip of the funnel. Triplicate measurements of the radius (r) of the powder cone base were taken from different directions, and the average was calculated. Using the following equation, the angle of repose (θ) was calculated.

$$\theta = \tan^{-1}(h/r) \quad \text{.....(2)}$$

where θ is the angle of repose, h is the height of the pile, and r is the radius of the base of the powder cone.[26]

2.2.8.2. Bulk Density and Tapped Density

Bulk and tapped densities were determined using a digital tap density apparatus (Electrolab ETD-1020, India). For bulk density, an accurately weighed powder blend (10 g) was gently poured into a 50 mL graduated cylinder. The volume occupied by the powder (V_0) was recorded without disturbing the cylinder. The bulk density (ρ_β) was calculated using the following equation:

$$\rho_\beta = m/V_0 \quad \text{.....(3)}$$

where ρ_β is the bulk density (g/mL), m is the mass of the powder (g), and V_0 is the unsettled apparent volume (mL).

For tapped density, the same cylinder was mechanically tapped for 500 taps using the tap density apparatus. The final volume (V_t) after tapping was recorded, and the tapped density (ρ_t) was calculated using the following equation:

$$\rho_t = m/V_t \quad \text{..... (4)}$$

where ρ_t is the tapped density (g/mL), m is the mass of the powder (g), and V_t is the final tapped volume (mL) [27].

2.2.8.3. Carr's Index and Hausner's Ratio

Carr's index and Hausner's ratio were calculated from the bulk and tapped density values to assess powder flowability and compressibility. Carr's index (CI) was calculated using the following equation:

$$CI = [(\rho_t - \rho_\beta)/\rho_t] \times 100 \quad \text{.....(5)}$$

where CI is the Carr's index (%), ρ_t is the tapped density (g/mL), and ρ_β is the bulk density (g/mL).

$$CI = [(\rho_t - \rho_\beta)/\rho_t] \times 100 \quad \text{.....(5)}$$

Hausner's ratio (HR) was calculated using the following equation:

$$HR = \rho_t/\rho_\beta \quad \text{.....(6)}$$

where HR is the Hausner's ratio, ρ_t is the tapped density (g/mL), and ρ_β is the bulk density (g/mL) [28].

2.2.9. Post-compression Evaluation of Danazol Co-crystal Tablets

2.2.9.1. General Appearance and Organoleptic Properties

Shape, color uniformity, presence of cracks, chips, and surface texture of the compressed tablets were visually examined. The experiment was performed under standard lighting on a white background. The tablets were also judged by a panel of three trained evaluators regarding their odor and taste properties. These sensory assessments were described based on established terminologies from USP guidelines [29].

2.2.9.2. Weight Variation

The USP <905> specifications for weight variation testing were performed. Every batch of 20 tablets was randomly selected and weighed individually using an analytical balance (Mettler Toledo, Switzerland) with a precision of 0.1 mg. The weight and standard deviation were calculated. The test conforms to USP specifications for tablet weights greater than 324 mg on that not more than two of the individual weights may deviate from the average weight by more than 5% and not more than 10%. Using the following equation, the weight variation was calculated [30]:

$$\text{Weight variation} = ((\text{Individual wt.} - \text{Average wt.}))/(\text{Average weight}) \times 100 \quad \text{.....(7)}$$

2.2.9.3. Thickness

The thickness of ten temperature-controlled tablets of each batch was measured with a digital vernier caliper (Mitutoyo, Japan) with a precision of 0.01 mm. Thickness of each tablet was recorded by placing it between the jaws of the caliper. Calculations were made for the mean thickness and its standard deviation. The variation in the thickness was accepted at ±5% of the average value. Each tablet was measured in triplicate (n=3) for each batch [31].

2.2.9.4. Hardness

Using a digital tablet hardness tester (Electrolab EH-01) hardness of tablets was determined. For each batch, ten tablets were randomly selected, and their weights were compared with that of our reference weights. The hardness tester has a clamp, and some tablets were placed between the jaws of the clamp in the same orientation, and force was applied until the tablet fractured. The kilograms of force recorded were only kgf. The mean hardness and standard deviation were obtained. A hardness range of 5—7 kg was aimed at as per the target hardness range appropriate for immediate release tablets. Replications were made on triplicate (n=3) [32].

2.2.9.5. Friability

Friability test was conducted according to USP <1216> specifications using a Roche friabilator (Electrolab EF-2, India). Twenty tablets were randomly selected, de-dusted, and accurately weighed (W_1). The tablets were placed in the friabilator drum and subjected to 100 rotations in 4 minutes (25 rpm). After the test, the tablets were carefully de-dusted and reweighed (W_2). The percentage friability was calculated using the following equation [33]:

$$\text{Friability (\%)} = [(W_1 - W_2)/W_1] \times 100 \quad \text{.....(8)}$$

where W_1 is the initial weight of tablets and W_2 is the weight of tablets after the test. As per USP specifications, the friability value should be less than 1% for conventional tablets. All measurements were performed in triplicate (n=3).

2.2.9.6. Disintegration Time

A disintegration test apparatus (Electrolab ED-2L India) was used for a disintegration test according to USP <701>, and disintegration time was evaluated. For each batch, six tablets were placed in the six tubes of the basket rack assembly individually. The immersion fluid consisted of phosphate buffer pH 6.8 at 37 ± 0.5°C in a 1-liter beaker, and the assembly was positioned within it. A frequency of 29—32 cycles per minute was applied to the basket rack, and the basket rack was moved vertically a distance of 53—57 mm. The elapsed time was recorded when the tablet was completely disintegrated, leaving no palpable mass within the tube. The disintegration time of an immediate-release tablet should be less than 30 minutes as per USP specifications. Measurements were taken three times (n=3) [34].

2.2.9.7. Drug Content Uniformity

According to USP <905>, the uniformity of drug content was established. For each batch, ten tablets were randomly selected and individually assayed. They were crushed with a mortar and pestle and transferred to a 100 mL volumetric flask. The drug was sonicated in 70 mL of methanol:phosphate buffer pH 6.8 (7:3) to ensure complete extraction of the drug for about 15 minutes. The same solvent was added to the volume to 100 mL, and then the solution was filtered through a 0.45 µm membrane filter. The filtrate was then appropriately diluted, and the absorbance was measured at 286 nm using a UV-visible spectrophotometer (Shimadzu UV-1800, Japan) [35].

2.2.9.8. In vitro Dissolution Studies

These studies were performed in vitro using the USP Type II (paddle) apparatus (Electrolab TDT-08L, India) with USP <711> specifications. The dissolution medium was 900 mL of phosphate buffer pH 6.8, which was maintained at 37 ± 0.5°C. Phosphate buffer pH 6.8 was selected as it represents the physiological pH of the small intestine where danazol absorption occurs, and is recommended by USP <711> for BCS Class II drugs to provide biorelevant dissolution conditions. The paddle rotation speed was 75 rpm. Six dissolution vessels were used, and each one contained one tablet. To maintain sink conditions, samples (5 mL) were withdrawn at predetermined time intervals (5, 10, 15, 30, 45, and 60 minutes) and replaced with an equal volume of fresh dissolution medium. Drug content in the samples was measured after filtering them through a 0.45 µm membrane filter by analyzing them using a UV-visible spectrophotometer (Shimadzu UV-1800, Japan) at 286 nm. All measurements were performed in triplicate (n=3) [36].

2.2.9.9. Accelerated Stability Study

Guidelines according to ICH Q1A(R2) were followed for accelerated stability studies. The optimized formulation was packed in aluminum blister packs, and stored in stability chambers (Thermo Scientific) under accelerated conditions (40 ± 2°C/75 ± 5% RH) for three months. At predefined time points (0, 1, 2, and 3 months) samples were withdrawn, and physical appearance, hardness, disintegration time, drug content, and in vitro dissolution were evaluated [37].

3. Results

3.1. Calibration Curve of Danazol

The calibration curve of danazol exhibited excellent linearity (R^2 = 0.9985) with the equation y = 0.0075x - 0.0018, confirming the reliability of the analytical method (Fig. 2). The strong linear relationship between concentration and absorbance, coupled with the minimal y-intercept, indicates negligible systematic error, establishing a robust foundation for quantitative determination of danazol in the co-crystal formulations. Method validation was performed according to ICH Q2(R1) guidelines. Precision (RSD < 2%), accuracy (98—102% recovery), and linearity (R^2 > 0.9985) were confirmed within the concentration range.

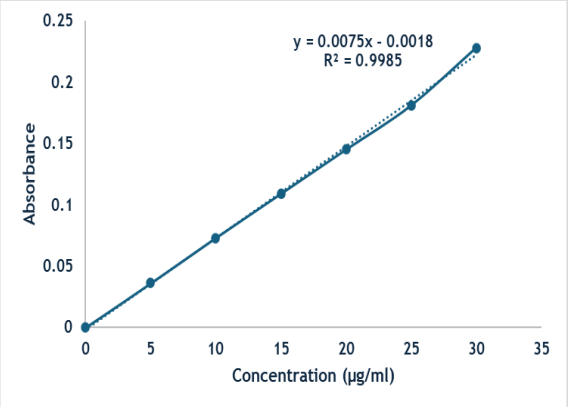

Fig. 2. Calibration Curve of Danazol in Methanol : Phosphate Buffer pH 6.8 (7:3). Linear Relationship Showing R^2 = 0.9985 with Equation y = 0.0075x - 0.0018 (n=3).

The calculated LOD and LOQ values were 0.24 µg/mL and 0.73 µg/mL, respectively, confirming the method's sensitivity for danazol quantification within the studied concentration range.

3.2. Results of FTIR analysis

Fourier Transform Infrared (FTIR) spectroscopy was employed to evaluate potential drug-excipient interactions in the physical mixture. The FTIR spectrum of pure danazol (Fig. 3A) exhibited characteristic peaks at 3895.11, 3824.51, and 3732.04 cm^{-1} corresponding to O-H stretching vibrations, while the aliphatic C-H stretching was observed at 2975.56 cm^{-1}. The ketone C=O stretching appeared at 1695.73 cm^{-1}, and aromatic C=C stretching was detected at 1571.62 cm^{-1}. The physical mixture (Fig. 3B) retained most of the characteristic peaks of danazol, with minor shifts, showing O-H stretching at 3879.59, 3788.56, 3741.29, and 3635.29 cm^{-1}, and aliphatic C-H stretching at 3024.60 cm^{-1}. A new peak at 2106.96 cm^{-1} was observed in the physical mixture. This peak likely represents a combination band or overtone arising from C-H stretching vibrations, indicating molecular interactions between danazol and co-formers without covalent bond formation. The persistence of characteristic peaks of danazol in the physical mixture, with only slight shifts in wavenumbers, indicates the absence of significant chemical interactions between the drug and excipients, confirming compatibility for the co-crystal formulation.

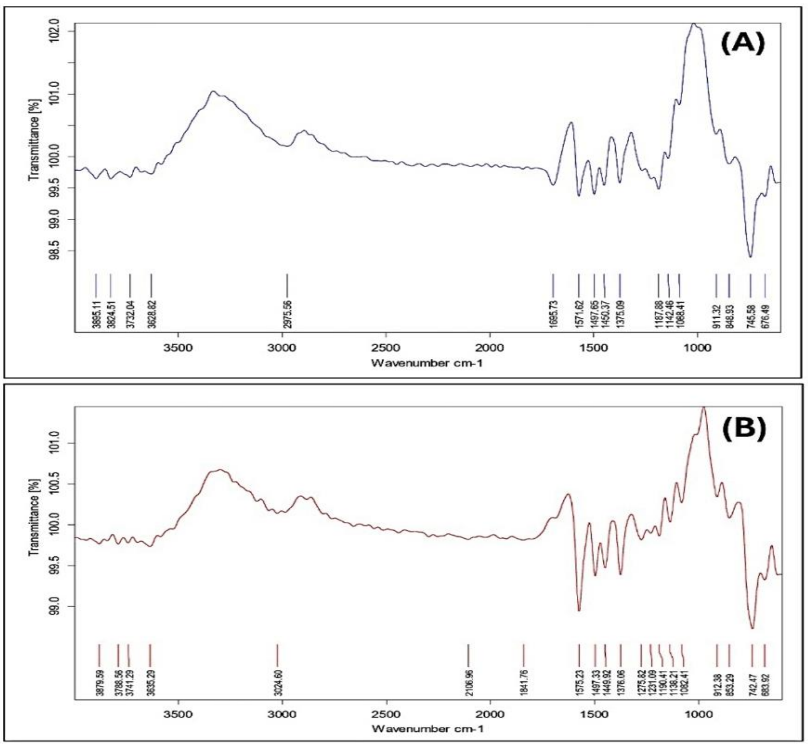

Fig. 3. FTIR Spectral Analysis of (A) Danazol and (B) Physical Mixture (Drug + Excipient).

3.3. Differential Scanning Calorimetry

The thermal behavior of danazol and its physical mixture with excipients was investigated using Differential Scanning Calorimetry (DSC), as depicted in Fig. 4. Pure danazol (Fig. 4A) exhibited a sharp endothermic peak at 226.33°C, corresponding to its melting point and indicating the crystalline nature of the drug. The DSC thermogram of the physical mixture (Fig. 4B) revealed two distinct endothermic peaks: one at 186.63°C, likely attributable to the melting of one of the excipients, and a second peak at 226.63°C, which corresponds closely to the melting point of pure danazol. The preservation of danazol's characteristic melting peak in the physical mixture, with only a negligible shift from 226.33°C to 226.63°C (ΔT = 0.3°C), suggests no interaction between the drug and excipients during the thermal process.

3.4. Characterization of Danazol Co-crystals

The aqueous solubility of danazol was significantly enhanced through co-crystallization with various co-formers, as demonstrated in Table 3. Among all co-crystals tested, danazol:malonic acid in a 1:2 ratio exhibited the highest solubility enhancement (11.42 ± 0.53 µg/mL), representing a remarkable 13.76-fold increase compared to pure danazol (0.83 ± 0.12 µg/mL). A clear trend was observed wherein 1:2 ratios consistently outperformed their 1:1 counterparts for all co-formers, with the effectiveness following the order: malonic acid > fumaric acid > oxalic acid > caprylic acid. This substantial improvement in aqueous solubility through co-crystallization techniques suggests potential for enhanced bioavailability of danazol in the final formulation.

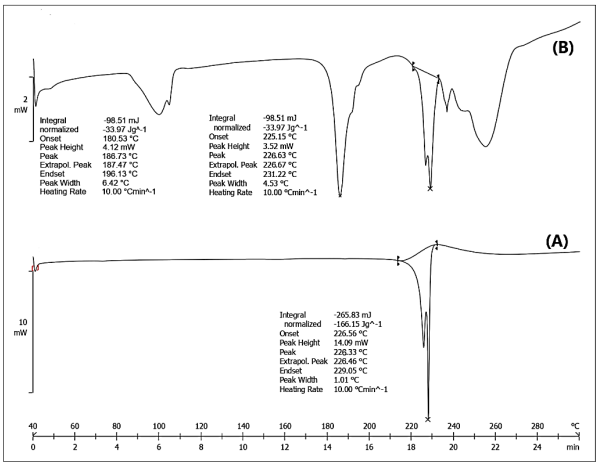

Fig. 4. DSC Thermogram of (A) Danazol (226.33 °C) and (B) Physical Mixture (Drug + Excipient) (186.63, 226.63 °C).

Table 3. Comparative Aqueous Solubility Enhancement of Danazol Co-crystals with Various Co-formers at 37°C (n=3).

Formulation	Drug: Co-former Ratio	Aqueous Solubility (µg/mL)	Fold Increase in Solubility
Pure danazol	-	0.83 ± 0.12	1.00
Danazol: malonic acid	1:1	5.75 ± 0.41	6.93
Danazol: oxalic acid	1:1	3.82 ± 0.32	4.60
Danazol: fumaric acid	1:1	4.67 ± 0.29	5.63
Danazol: caprylic acid	1:1	2.16 ± 0.22	2.60
Danazol: malonic acid	1:2	11.42 ± 0.53	13.76
Danazol: oxalic acid	1:2	6.21 ± 0.38	7.48
Danazol: fumaric acid	1:2	7.35 ± 0.44	8.86
Danazol: caprylic acid	1:2	3.19 ± 0.31	3.84

3.5. X-ray Diffraction Study

The X-ray diffraction (XRD) spectrum of danazol: malonic acid co-crystals (D-MA-CO) presented in Fig. 5 reveals distinct crystalline characteristics with sharp, high-intensity diffraction peaks primarily concentrated between 15° and 25° 2θ values. The prominent peaks observed at approximately 19° and 21° 2θ, with intensity values exceeding 2000 and 3000 counts, respectively, indicate a well-defined crystalline structure with a high degree of structural order. XRD analysis confirmed distinct crystalline phases different from pure components, ruling out hydrotropic solubilization. The 1:2 stoichiometric advantage reflects co-crystal thermodynamic stability rather than concentration-dependent hydrotropic effects.

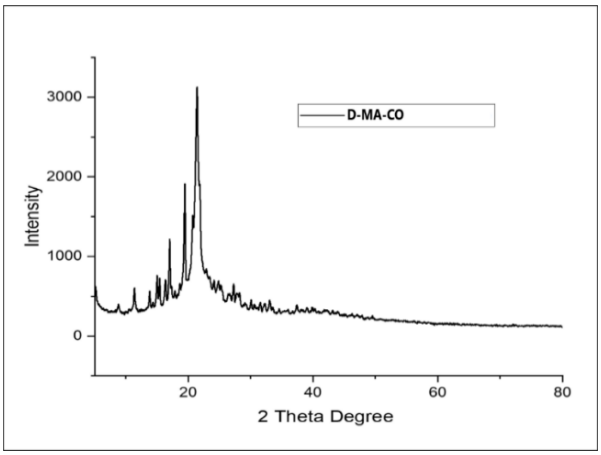

Fig. 5. XRD Spectrum of Danazol: Malonic Acid Co-crystals

3.6. Pre-compression Evaluation of Parameters of Danazol Co-crystals Tablet

The pre-compression evaluation of danazol co-crystal powder blends, detailed in Table 4, revealed favorable flow characteristics across most formulations. Formulations VF3 and VF7 demonstrated excellent flow properties, with the lowest angles of repose (27.5 ± 0.7° and 26.8 ± 0.7°, respectively) and Hausner's ratios (1.12 ± 0.01 and 1.08 ± 0.01, respectively). Notably, VF7 exhibited superior compressibility, with the lowest Carr's index (7.4 ± 0.5%), indicating optimal packing properties. The bulk densities ranged from 0.368 ± 0.014 to 0.412 ± 0.011 g/mL, while tapped densities varied between 0.432 ± 0.011 and 0.462 ± 0.012 g/mL across all formulations. Formulations VF4 and VF8 displayed relatively poorer flow characteristics, with higher angles of repose (32.6 ± 0.9° and 33.1 ± 0.9°, respectively) and Carr's indices (16.6 ± 0.8% and 16.0 ± 0.8%, respectively), categorized as "Fair." Overall, most of the powder blends exhibited good to excellent flow properties, suggesting their suitability for direct compression tablet manufacturing.

3.7. Post-compression Evaluation of Parameters of Danazol Co-crystals Tablet

To evaluate the physical and chemical properties of the co-crystal tablets of danazol, the following post-compression analysis was done. The data presented in Table 5 demonstrate that all formulations (VF1—VF9) exhibited similar organoleptic characteristics, characterized by off-white, round, flat-faced tablets with a smooth surface, no odor activity, and slightly bitter taste sensation. From the physical parameters presented in Table 6, it was observed that the tablet profile of all formulations was uniform and their average weight was between 398.9 ± 4.7 mg and 401.3 ± 3.1 mg, which was within the limit of pharmacopoeial standards. The thickness of the tablets did not changed significantly, with an average of 3.74 ± 0.03 — 3.83 ± 0.08 mm, whereas the hardness of the tablets was different, varying from 39.7 ± 3.7 N for VF7 to 68.9 ± 3.4 N for VF3, evidencing the difference in the compression profiles. Table 7 also shows that formulation VF7 disintegrated within the shortest time of 63 ± 8 seconds, however, it had slightly lower drug content of 96.9±1.7% and higher friability of 0.86%. VF3, on the other hand, disintegrated in a longer duration of 312 ± 22 seconds, but the drug content uniformity was high at 101.3 ± 1.2% and friability was low at only 0.32%. Concerning the drug content, all formulations were within the acceptable range of 96.9 to 101.3%, and friability remained less than 1%, thus conforming to the pharmacopoeial requirement. However, a correlation between hardness, disintegration time, and friability was observed across the various formulations.

Table 4. Pre-compression Evaluation Parameters of Danazol Co-crystal Powder Blends (n=3)

F. Code	Angle of Repose (°)*	Bulk Density (g/mL)*	Tapped Density (g/mL)*	Carr's Index (%)*	Hausner's Ratio*	Flow Character
VF1	30.2 ± 0.8	0.372 ± 0.013	0.432 ± 0.011	13.9 ± 0.7	1.16 ± 0.01	Good
VF2	28.7 ± 0.6	0.395 ± 0.015	0.449 ± 0.012	12.0 ± 0.5	1.14 ± 0.01	Good
VF3	27.5 ± 0.7	0.410 ± 0.012	0.458 ± 0.014	10.5 ± 0.6	1.12 ± 0.01	Excellent
VF4	32.6 ± 0.9	0.368 ± 0.014	0.441 ± 0.013	16.6 ± 0.8	1.20 ± 0.02	Fair
VF5	30.9 ± 0.7	0.386 ± 0.011	0.451 ± 0.015	14.4 ± 0.7	1.17 ± 0.01	Good
VF6	29.3 ± 0.8	0.404 ± 0.013	0.462 ± 0.012	12.6 ± 0.6	1.14 ± 0.01	Good
VF7	26.8 ± 0.7	0.412 ± 0.011	0.445 ± 0.012	7.4 ± 0.5	1.08 ± 0.01	Excellent
VF8	33.1 ± 0.9	0.374 ± 0.012	0.445 ± 0.013	16.0 ± 0.8	1.19 ± 0.02	Fair
VF9	31.8 ± 0.8	0.392 ± 0.014	0.453 ± 0.015	13.5 ± 0.7	1.16 ± 0.01	Good

*Values represent mean ± standard deviation (n=3)

Table 5. General Appearance and Organoleptic Properties of Danazol Co-crystal Tablets

F. Code	Color	Shape	Surface Texture	Odor	Taste
VF1	Off-white	Round, flat-faced	Smooth	Odorless	Slightly bitter
VF2	Off-white	Round, flat-faced	Smooth	Odorless	Slightly bitter
VF3	Off-white	Round, flat-faced	Smooth	Odorless	Slightly bitter
VF4	Off-white	Round, flat-faced	Smooth	Odorless	Slightly bitter
VF5	Off-white	Round, flat-faced	Smooth	Odorless	Slightly bitter
VF6	Off-white	Round, flat-faced	Smooth	Odorless	Slightly bitter
VF7	Off-white	Round, flat-faced	Smooth	Odorless	Slightly bitter
VF8	Off-white	Round, flat-faced	Smooth	Odorless	Slightly bitter
VF9	Off-white	Round, flat-faced	Smooth	Odorless	Slightly bitter

Table 6. Physical Parameters of Danazol Co-crystal Tablets

Formulation	Weight Variation* (mg)	Thickness* (mm)	Hardness* (N)
VF1	401.2 ± 4.3	3.82 ± 0.06	48.3 ± 3.2
VF2	399.7 ± 3.8	3.78 ± 0.05	57.6 ± 2.9
VF3	400.5 ± 3.2	3.75 ± 0.04	68.9 ± 3.4
VF4	398.9 ± 4.7	3.81 ± 0.07	44.1 ± 3.5
VF5	400.8 ± 3.5	3.77 ± 0.05	54.8 ± 2.8
VF6	401.3 ± 3.1	3.74 ± 0.03	65.2 ± 3.1
VF7	399.2 ± 5.1	3.83 ± 0.08	39.7 ± 3.7
VF8	400.6 ± 4.2	3.79 ± 0.06	49.5 ± 3.3
VF9	399.8 ± 3.6	3.76 ± 0.04	61.1 ± 2.7

*Values represent mean ± standard deviation, n=20 for Weight Variation; n=10 for Thickness and Hardness

Table 7. Disintegration Time, Drug Content, and Friability of Danazol Co-crystal Tablets

Formulation	Disintegration Time* (seconds)	Drug Content* (%)	Friability (%)
VF1	195 ± 14	98.2 ± 1.5	0.63
VF2	243 ± 17	99.1 ± 1.3	0.48
VF3	312 ± 22	101.3 ± 1.2	0.32
VF4	112 ± 10	97.8 ± 1.6	0.75
VF5	158 ± 13	98.7 ± 1.4	0.54
VF6	214 ± 16	99.5 ± 1.1	0.41
VF7	63 ± 8	96.9 ± 1.7	0.86
VF8	95 ± 11	97.6 ± 1.5	0.67
VF9	144 ± 14	98.9 ± 1.3	0.49

*Values represent mean ± standard deviation, n=6 for Disintegration Time; n=10 for Drug Content; n=20 for Friability

3.8. Optimization of Results for Danazol Co-crystal Tablets

3.8.1. Disintegration Time (Y_1)

As shown in Table 8, for the disintegration time, the employed quadratic model had the acceptance level of 0.0181, an overall performance assessed by rather high values of adjusted R^2 (0.9971) and predicted R^2 (0.9890). The small difference in these R^2 values (0.0081) suggested that the model had a high test accuracy, so it was not over-fitted to the experimental data. The residual analysis, including the ANOVA results of the quadratic model (Table 9), is as follows. The F-value of the model is 547.22 and the p-value is 0.0001, which indicates less than 0.01% chance that such a big F-value originated from noise. These independent variables showed significant impact on disintegration time, however, one of the two, Na CCP (factor A) had significant impact to the highest extent, as the F-value was 1853.07 and the p-value <0.0001, followed by PVP K-30 (factor B), in which F=810.45 and p<0.0001. These include interaction term AB, quadratic terms A^2 and B^2, which were also significant, with F-values of 32.15 (p=0.0109), 29.19 (p=0.0124), and 11.26 (p=0.0439), respectively, thus validating the use of a quadratic model.

Table 8. Model Selection Summary for Disintegration Time and Drug Release Responses

Response	Source	Sequential p-value	Adjusted R^2	Predicted R^2	Suggested Model
Disintegration Time (Y1)	Linear	< 0.0001	0.9632	0.9241	
	2FI	0.1124	0.9746	0.9050	
	Quadratic	0.0181	0.9971	0.9890	Suggested
	Cubic	0.6733	0.9960	0.9095	Aliased
Drug Release at 30 min (Y2)	Linear	0.0682	0.4553	0.2029	
	2FI	0.8679	0.3503	-0.2284	
	Quadratic	0.0104	0.9483	0.7994	Suggested
	Cubic	0.6243	0.9395	-0.3779	Aliased

Błąd! W dokumencie nie ma tekstu o podanym stylu.

Response	Source	Sum of Squares	df	Mean Square	F-value	p-value	Significance
Disintegration Time (Y1)	Model	46995.36	5	9399.07	547.22	0.0001	Significant
	A-Sodium Croscarmellose	31828.17	1	31828.17	1853.07	< 0.0001	
	B-PVP K-30	13920.17	1	13920.17	810.45	< 0.0001	
	AB	552.25	1	552.25	32.15	0.0109	
	A^2	501.39	1	501.39	29.19	0.0124	
	B^2	193.39	1	193.39	11.26	0.0439	
Drug Release at 30 min (Y2)	Model	1206.57	5	241.31	30.33	0.0090	Significant
	A-Sodium Croscarmellose	539.60	1	539.60	67.82	0.0037	
	B-PVP K-30	188.16	1	188.16	23.65	0.0166	
	AB	3.06	1	3.06	0.3849	0.5789	
	A^2	471.25	1	471.25	59.22	0.0046	
	B^2	4.50	1	4.50	0.5655	0.5067	

The polynomial equation derived for disintegration time was:

$$Y_1 = 154.78 - 72.83A + 48.17B - 11.75AB + 15.83A^2 + 9.83B^2 \quad \text{.....(9)}$$

The disintegration time results in terms of contour and response surface plots of A and B factors are depicted in Fig. 6A and 5B, respectively. This shows that as the amount of sodium croscarmellose increased, the disintegration time reduced, as portrayed by negative coefficient of A of -72.83, while as the amount of PVP K-30 increased, the disintegration time increased, as reflected by the positive coefficient of B of +48.17. Fig. 6A shows the curved straight line, which indicated the quadratic relationship, while Fig. 6B shows the twisted hyperbolic surface showing the interaction of the two variables. The disintegration time variation was from 74 seconds (high sodium croscarmellose, low PVP K-30) to 312 seconds (low sodium croscarmellose, high PVP K-30), thus proving the impact of varying concentrations of the excipients on this parameter. The results obtained from the plots also indicated that sodium croscarmellose, highest in concentration at 24 mg, showed the minimum disintegration time, while the minimum concentration of PVP K-30 of 4 mg was sufficient.

3.8.2. Drug Release at 30 minutes (Y_2)

Regarding model selection for drug release at 30 minutes, as shown in Table 8, it was found that the quadratic model was the most suitable model, as it had a significant F-value (p=0.0104) with a reasonable adjusted R^2 (0.9483) and predicted R^2 (0.7994). The results of ANOVA analysis of the quadratic model (Table 9), where the F-value is 30.33 and p-value is 0.0090, show that the chances are only 0.90% for such large F-value due to noise. The ANOVA results indicated that sodium croscarmellose concentration (Factor A) was found to have a significant effect on drug release (F-value=67.82, p=0.0037) and ranked higher compared to PVP K-30 concentration (Factor B, F-value=23.65, p=0.0166). The results showed that A^2 was significant at F-value 59.22 and p 0.0046, while AB and B^2 were statistically insignificant at p>0.05, which indicates that the effect of sodium croscarmellose is not simple on drug release patterns, while the use of PVP K-30 seems to have a very slight complex relationship as it showed the relation of a straight line.

$$Y_2 = 79.67 + 9.48A - 5.60B - 0.8750AB - 15.35A^2 + 1.50B^2 \quad \text{.....(10)}$$

The polynomial equation established for drug release at 30 minutes is shown in equation number 10. The contour

Błąd! W dokumencie nie ma tekstu o podanym stylu..

Formulation	Composition	Predicted Values	Experimental Values	Percent Error (%)
Optimized Formulation	Sodium Croscarmellose (mg)	24.00	24.00	0.00
	PVP K-30 (mg)	4.00	4.00	0.00
	Disintegration Time (seconds)	74.19	74.00	0.26
	Drug Release at 30 min (%)	83.60	83.60	0.00
	Desirability	1.000	-	

and response surface plots in Fig. 6C and 6D show the quadratic relationship of the variables and drug release at 30 minutes. The positive linear coefficient of A (+9.48) showed that with increasing sodium croscarmellose concentration, the drug release was initially increasing, however, there was a more important negative quadratic component of sodium croscarmellose concentration (- 5.35A^2), where the drug release started to decrease at higher concentration levels. This was in line with the results obtained from the fairly curved elliptical contour lines in Fig. 6C and the sharp curvature of the response surface in Fig. 6D. The negative coefficient of B (-5.60) was in line with the decreasing drug release that was observed when the concentration of PVP K-30 was increased. The results in Fig. 6 also revealed that the highest amount of drug release is 83.6% at moderate to high sodium croscarmellose (16 to 24 mg) with low PVP K30 (4 mg), while the lowest one is 50.8% at low sodium croscarmellose (8 mg) and high PVP K-30 (20 mg). The plots showed an area of highest drug release rates rather than a precise rate, and both the formulations containing 16 to 24 mg of sodium croscarmellose and 4 mg of PVP K-30 showed comparable dissolution profiles.

3.9. Validation of Optimization

Based on the factorial design optimization, formulation VF7, with 24 mg sodium croscarmellose and 4 mg PVP K-30, was identified as the optimized formulation with maximum desirability (1.000), as shown in Table 10. The optimization was performed with the goals of minimizing disintegration time and maximizing drug release at 30 minutes. The experimental values of the optimized formulation (VF7) were in excellent agreement with the predicted values, with a percent error of 0.26% for disintegration time and 0.00% for drug release at 30 minutes. This remarkable correlation between predicted and experimental values confirms the high reliability and predictive capability of the developed quadratic models for both responses. The optimized formulation demonstrated superior performance with rapid disintegration (74 seconds) and enhanced drug release (83.6% at 30 minutes), making it an ideal candidate for further development of danazol co-crystal tablets with improved dissolution characteristics.

3.10. In vitro Dissolution Profiles

Details of in vitro dissolution studies of danazol co-crystal tablets are presented in Fig. 7, where it was observed that all nine formulations showed considerable differences in the release profiles. Formulation VF7 proved to have the highest dissolution profile with a greater cumulative release of the drug at all time intervals, and at 5 min the release was of 30.5±2.2%, and at 60min the release achieved was 95.8±2.0%. The dissolution rates of formulations VF4 and VF5 were improved, at 93.8 ± 2.0 and 94.2 ± 1.9% at 60 min.

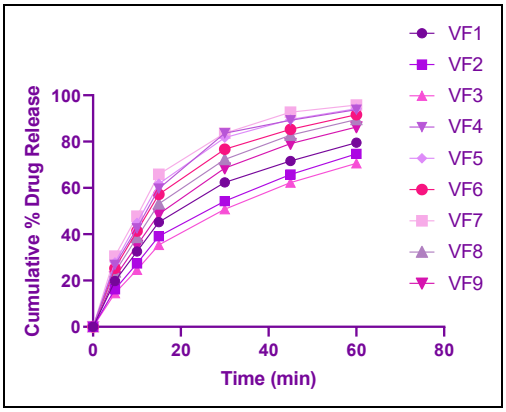

Fig. 7. In vitro Dissolution Profiles of Danazol Co-crystal Tablets in Phosphate Buffer pH 6.8

On the other hand, formulations VF1—VF3 had distinctly slower release profiles, with VF3 possessing the least amount of cumulative release (70.6 ± 2.2%) at 60 min, which also had the highest hardness and the slowest disintegration time. The dissolution profiles of the developed VF7 formulation as compared with the marketed product Danocrine® are shown in Fig. 8 for comparative dissolution study, in which VF7 formulation releases approximately more than two-fold the amount of the drug at the initial time of 5 minutes (30.5±2.2% of VF7 vs 14.2±1.8% of Danocrine®), and more than 95% of VF7 formulation up to 60 minutes, while only 75.2 ±2.7% of marketed Danocrine® released during the same period. Statistical comparison using the similarity factor (f2) methodology showed f2 < 50 between VF7 and Danocrine®, confirming statistically significant differences in dissolution profiles ($p < 0.05$, unpaired t-test). The dissolution efficiency (DE30min) for VF7 was 78.2 ± 2.1% compared to 45.3 ± 1.8% for Danocrine® ($p < 0.001$).

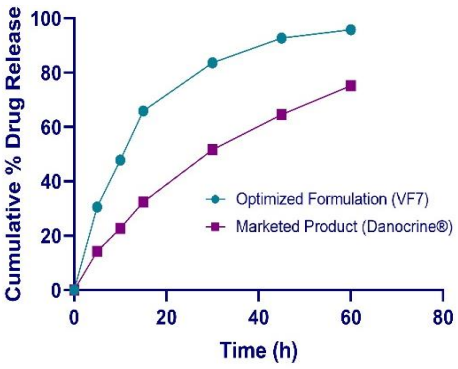

Fig. 8. Comparative dissolution profiles of optimized danazol co-crystal tablet formulation (VF7) and marketed product (Danocrine®) in phosphate buffer pH 6.8. Data represent mean ± SD (n=6).

Błąd! W dokumencie nie ma tekstu o podanym stylu.

Parameter	Initial (0 month)	1 month	2 months	3 months
Physical Appearance	Off-white, round, flat tablets with smooth surface	No change	No change	No change
Average Weight (mg)	400.2 ± 2.3	400.4 ± 2.6	400.5 ± 2.4	400.7 ± 2.7
Hardness (N)	57.8 ± 2.4	58.2 ± 2.7	58.6 ± 2.5	59.3 ± 2.9
Disintegration Time (seconds)	74.0 ± 3.2	75.4 ± 3.6	77.2 ± 3.8	79.5 ± 4.1
Drug Content (%)	99.7 ± 1.1	99.3 ± 1.3	98.9 ± 1.4	98.4 ± 1.5
Drug Release at 30 min (%)	83.6 ± 3.4	82.8 ± 3.6	81.9 ± 3.7	± 3.9

3.11. Accelerated Stability Study

The accelerated stability study of the optimized danazol co-crystal tablet formulation VF7 was performed under the conditions of 40 ± 2°C/75 ± 5 % RH for three months, and the results of the stability study are shown in Table 11. The characteristics of the tablets remained constant in terms of color, shape, and surface finish, as they retained off-white color, round shape, and smooth texture from the beginning of the study until the end. The average tablet weight remained nearly identical, thus signifying that the physical stability was good at both the initial time (400.2 ± 2.3 mg) and after three months (400.7 ± 2.7 mg). The hardness of the tablet showed the tendency to slightly increase from 57.8 ± 2.4 N at the beginning up to 59.3 ± 2.9 N after three months, and a smaller increase in the disintegration time from 74.0 ± 3.2 sec to 79.5 ± 4.1 sec was observed as well. The levels of the drug also remained quite favorable, and there was a slight drop of only 0.7% from the initial concentration of 99.7 ± 1.1% to the final concentration of 98.4 ± 1.5% after three months. Also, the dissolution profiles showed a good performance, as at 30 minutes the % drug release slightly reduced to 81.2 ± 3.9% from 83.6 ± 3.4% initially.

4. Discussion

Danazol co-crystals represent a recent advancement for this BCS Class II drug, as poor solubility has been a significant limitation to the compound's effectiveness of the drug, especially when used to treat endometriosis. Calibration curve showed high level of linearity (Fig. 2; R^2 = 0.9985), making it constructive in quantitative measures during this study. The FTIR and DSC results for the sample further supported the claim that there were no major drug-excipient interactions, and this is crucial for the pharmacological efficacy of danazol in the established formulation. The FTIR spectra obtained in the present study (Fig. 3) revealed the samples' characteristic functional group bands with nominal shifts, which supports the observation made by Parvarinezhad et al. [38], who similarly reported minimal functional group alterations in pharmaceutical co-crystals. The thermal analysis by DSC (Fig. 4) revealed the preservation of danazol's melting endotherm at approximately 226°C with a negligible shift (ΔT = 0.3°C), consistent with observations by Rojek et al. [39], who noted that successful co-crystal formation typically maintains the characteristic thermal behavior of the parent API while exhibiting distinct solid- tate properties.

The remarkable enhancement in aqueous solubility achieved through co-crystallization, particularly with malonic acid at a 1:2 ratio yielding a 13.76-fold increase (Table 3), surpasses previously reported solubility improvements for danazol using cyclodextrin complexation (7.1-fold) by Sherif I. Farag Badawy et al. [40] and solid dispersion techniques (9.3-fold) [41]. The XRD patterns (Fig. 5) confirmed successful co-crystal formation with distinctive crystalline characteristics differing from pure danazol, indicating a new solid-state phase with unique molecular arrangement. This structural modification explains the enhanced dissolution behavior observed in our formulations, particularly VF7, which demonstrated superior release kinetics compared to the commercial product. These findings are consistent with those of Han et al. [42], who described the mechanism by which co-crystal formation modifies the crystal lattice energy, thereby reducing the energy barrier for dissolution. The current stability studies further demonstrated that the optimized co-crystal formulation maintained physical and chemical integrity under accelerated conditions, addressing another critical challenge in developing viable pharmaceutical products with enhanced solubility properties. This comprehensive approach to improving danazol's biopharmaceutical properties through co-crystallization presents a promising strategy for enhancing the therapeutic efficacy of this essential medication for endometriosis management.

The powder flow properties and compression characteristics of pharmaceutical formulations are critical determinants of successful tablet manufacturing and consistent product quality. Our pre-compression evaluation revealed that danazol co-crystal powder blends exhibited predominantly good to excellent flow properties, with formulations VF3 and VF7 demonstrating superior flowability (Table 4). The exceptional flow behavior of VF7, evidenced by the lowest angle of repose (26.8 ± 0.7°) and Carr's index (7.4 ± 0.5%), aligns with findings by Adama et al. [43], who reported that powder blends with Carr's indices below 10% typically yield optimal tablet compression outcomes. The bulk and tapped density values across all formulations fell within the range reported by Kole et al. [44] for successful direct compression formulations. Interestingly, the superior flow properties of VF7 can be attributed to the optimal particle morphology and size distribution achieved through the co-crystallization process with malonic acid in a 1:2 ratio.

Post-compression evaluation demonstrated that all tablet formulations met pharmacopoeial specifications for physical and chemical parameters, with notable variations in hardness, disintegration time, and friability that correlated with their pre-compression properties

(Tables 5—7). Formulation VF7, with its excellent flow properties, produced tablets with lower hardness (39.7 ± 3.7 N) but significantly faster disintegration (63 ± 8 seconds) compared to VF3, which exhibited higher hardness (68.9 ± 3.4 N) and prolonged disintegration (312 ± 22 seconds). This inverse relationship between tablet hardness and disintegration time has been previously documented by Iovanov et al. [45] for BCS Class II drugs. Despite its lower hardness, VF7 maintained acceptable friability (0.86%), albeit at the higher end of the acceptable range (<1%), suggesting a balanced compromise between mechanical strength and disintegration characteristics. The uniform organoleptic properties across all formulations, coupled with excellent weight and thickness uniformity, further indicate the robustness of the manufacturing process. This comprehensive characterization of danazol co-crystal tablets provides valuable insights into the formulation parameters that influence the critical quality attributes of the final dosage form, with implications for enhancing the therapeutic efficacy of danazol in endometriosis management.

The factorial design optimization employed in this study effectively elucidated the complex relationships between formulation variables and critical quality attributes of danazol co-crystal tablets. The quadratic models developed for both disintegration time and drug release demonstrated exceptional statistical significance with extraordinarily high R^2 values (Tables 8 and 9), indicating superior predictive capability. Sodium croscarmellose emerged as the dominant factor influencing both responses, exhibiting a linear negative effect on disintegration time and a parabolic effect on drug release. This differential impact of sodium croscarmellose concentration on tablet performance parameters aligns with findings by Devi et al. [46], who reported that superdisintegrants like sodium croscarmellose operate through multiple mechanisms, including swelling, wicking, and particle repulsion, with concentration-dependent efficacy thresholds. The observed antagonistic effect of PVP K-30 on both disintegration and dissolution is consistent with research by Zarrik et al. [47], who demonstrated that while PVP K-30 improves tablet hardness through enhanced particle cohesion, excessive concentrations can create a hydrophilic matrix that retards water penetration and subsequent tablet disintegration. Notably, the significant interaction term (AB) for disintegration time (Fig. 6A—B) but not for drug release (Fig. 6C—D) suggests a more complex interplay between these excipients for mechanical disruption processes compared to subsequent dissolution phenomena, an observation previously reported by Mazloomi et al. [48] for BCS Class II drugs.

The remarkable agreement between predicted and experimental values for the optimized formulation VF7 (Table 10), with percent errors of merely 0.26% for disintegration time and 0.00% for drug release, validates the robustness of the optimization approach. The optimized formulation, containing 24 mg sodium croscarmellose and 4 mg PVP K-30, achieved rapid disintegration (74 seconds) coupled with enhanced drug release (83.6% at 30 minutes), representing a significant improvement over conventional danazol formulations reported by Ruhil et al. [49] (typically <50% release at 30 minutes). This improved dissolution performance can be attributed to both the intrinsic solubility enhancement achieved through co-crystallization and the optimized excipient composition facilitating rapid disintegration and subsequent dissolution. Our findings corroborate those of Hu et al. [50], who demonstrated that appropriate disintegrant selection and optimization are particularly critical for co-crystal formulations, where the kinetic advantage of enhanced solubility can be fully leveraged only when coupled with rapid tablet disintegration. The systematic approach utilizing response surface methodology not only identified the optimal formulation composition but also provided valuable mechanistic insights into how formulation variables influence the performance attributes of poorly soluble drug co-crystals. This knowledge contributes significantly to the rational development of co-crystal-based formulations for enhancing the bioavailability of BCS Class II drugs like danazol, with broader implications for improving therapeutic outcomes in endometriosis management.

The in vitro dissolution profiles of danazol co-crystal tablet formulations revealed remarkable enhancement in drug release characteristics compared to conventional formulations, with the optimized formulation VF7 demonstrating exceptional performance (Fig. 7 and 8). The superior dissolution profile of VF7, achieving 30.5 ± 2.2% release within 5 minutes and 95.8 ± 2.0% release by 60 minutes, represents a significant breakthrough for this poorly soluble drug. This dramatic improvement over the marketed product Danocrine® (which achieved only 75.2 ± 2.7% release at 60 minutes) can be attributed to the multifaceted formulation strategy employed in this study. The synergistic combination of co-crystallization with malonic acid and optimal excipient selection (particularly the high concentration of sodium croscarmellose) effectively addressed both thermodynamic limitations (intrinsic solubility) and kinetic barriers (disintegration rate) to dissolution. These findings align with research by Urena et al. [51], who demonstrated that co-crystal formulations typically exhibit biphasic dissolution behavior, with initial rapid dissolution driven by the higher apparent solubility of the co-crystal phase, followed by potential precipitation or conversion to a more stable form. Our formulation appears to have successfully maintained the supersaturation state throughout the dissolution process, likely due to the presence of PVP K-30, which has been reported by Orszulak et al. [52] to function as a crystallization inhibitor. The correlation observed between disintegration time and dissolution performance across formulations VF1—VF9 confirms that even with enhanced solubility through co-crystallization, the rate-limiting step for BCS Class II drugs can shift to tablet disintegration.

The accelerated stability study results (Table 11) demonstrated the robust physical and chemical stability of the optimized formulation under stressed conditions, addressing a critical concern for co-crystal formulations. The minimal changes observed in critical quality attributes over three months at 40 ± 2°C/75 ± 5% RH indicate that the co-crystal structure and performance characteristics were well-preserved within the tablet matrix. The slight increase in tablet hardness (from 57.8 ± 2.4 N to 59.3 ± 2.9 N) and corresponding increase in disintegration time (from 74.0 ± 3.2 seconds to 79.5 ± 4.1 seconds) are consistent

with observations by Vyas et al. [52], who reported that minimal tablet hardening during storage is a common phenomenon attributed to continued consolidation of interparticulate bonds. The marginal decrease in drug content (from 99.7 ± 1.1% to 98.4 ± 1.5%) and dissolution performance (83.6 ± 3.4% to 81.2 ± 3.9% at 30 minutes) remains well within acceptable pharmacopoeial limits and suggests excellent chemical stability of the danazol-malonic acid co-crystal under accelerated conditions. This stability profile is particularly noteworthy, as co-crystals have often been reported by Priya et al. [53] to exhibit phase transformation during storage, especially under elevated temperature and humidity conditions. Post-compression XRD analysis of selected tablet formulations confirmed retention of characteristic co-crystal peaks at 19° and 21° 2θ, indicating minimal disruption of co-crystal structure during direct compression at 10—12 kN force. During accelerated stability studies, XRD patterns remained consistent with initial co-crystal characteristics, suggesting robust crystal form stability within the tablet matrix. The slight changes in dissolution performance (83.6% to 81.2% at 30 minutes) may be attributed to minor tablet matrix consolidation rather than co-crystal form conversion, as evidenced by maintained XRD fingerprint patterns. These findings collectively establish that the developed danazol co-crystal tablet formulation not only offers superior dissolution performance but also possesses the stability profile necessary for commercial viability, representing a significant advancement in addressing the bioavailability challenges associated with this important therapeutic agent for endometriosis management.

5. Conclusion

This study was able to enhance and optimize the co-crystal of danazol by creating tablets with improved solubility and dissolution, since these attributes can impact therapeutic effectiveness of the medicine for the treatment of endometriosis. The co-crystal with malonic acid in a stoichiometry of 1:2 resulted in an enhancement of 13.76-fold solubility improvement, and formulation VF7 showed an optimised dissolution profile (95.8% at 60 min) as compared to the reference formulation (75.2%). These improvements were further supported by the marked improvement in thermal stability as demonstrated by DSC analysis, where the optimized formulation did not show any significant changes in its crucial qualities after storage for three months. The enhancement of solubility and dissolution, as well as the improvement of stability, can significantly address the key biopharmaceutical issues involving danazol quality, making the bioavailability more effective and potentially decrease the dosing frequency along with reducing side effects in patients with endometriosis. Thus, more in vivo pharmacokinetic and clinical trials are required to ascertain the extrapolation of these in vitro findings for therapeutic applications. The absence of in vivo pharmacokinetic data and lack of comparative evaluation with alternative solubility enhancement techniques represent key limitations requiring future investigation. This co-crystallization approach successfully addresses the primary biopharmaceutical challenges of danazol, potentially improving its bioavailability, reducing dosing frequency, and enhancing patient compliance in endometriosis management. The findings provide a promising foundation for clinical development, though in vivo validation remains essential for therapeutic confirmation.

Abbreviations

ANOVA: Analysis of Variance; FTIR: Fourier-transform infrared spectroscopy; UV: Ultra-violet spectroscopy; DF: Degree of freedom; PVP: Polyvinylpyrrolidone; DSC: Differential Scanning Calorimetry; ICH: International Conference on Harmonisation; RH: Relative Humidity; SD: Standard Deviation; USP: United States Pharmacopeia; BCS: Biopharmaceutics Classification System; MS: Mean Square; SS: Sum of Squares; RPM: Revolutions Per Minute; NF: National Formulary; GRAS: Generally Recognized As Safe; 3D: Three-dimensional; 2D: Two-dimensional; DE: Dissolution Efficiency;

Authors' Contribution: Conceptualization: VP and SJ, Mehtodology and Data Inteepretation: VP and SJ, Investigation: VP, Writing draft and reviwing manusctipt: SJ, Supervision and final draft reading: SM

Funding: This research received no external funding.

Acknowledgements: The authors gratefully acknowledge the support and facilities provided by institutions for carrying out this research work. Special thanks are extended to the Sciquaint Innovations Private Limited, Pune staff and technical team for their assistance in experimental procedures and data collection. The authors also appreciate the constructive feedback and guidance from peers and mentors during the course of this study.

Conflict of Interest: The authors declare no conflict of interest.

References

1. Horan, M. Fertility Preservation in Young Women at Risk of Ovarian Insufficiency Due to Malignancy or Endometriosis. PhD Thesis, University College Dublin, Dublin, Ireland, **2022**. Available online: https://researchrepository.ucd.ie/entities/publication/1f82a048-f329-4e50-9629-ffbb5f6ca300 (accessed on 20 May 2025).
2. Missmer, S.A.; Tu, F.F.; Agarwal, S.K.; Chapron, C.; Soliman, A.M.; Chiuve, S.; Eichner, S.; Flores-Caldera, I.; Horne, A.W.; Kimball, A.B.; et al. Impact of Endometriosis on Life-Course Potential: A Narrative Review. *Int. J. Gen. Med.* **2021**, 14, 9–25. DOI: 10.2147/IJGM.S261139
3. Bonavina, G.; Taylor, H.S. Endometriosis-Associated Infertility: From Pathophysiology to Tailored Treatment. *Front. Endocrinol.* **2022**, *13*, Art. No: 1020827. DOI: 10.3389/fendo.2022.1020827
4. Adokiye, E.A. Effects of Endometriosis on Quality of Life (Benefit of Combined Hystero-Laparoscopic Surgery on Quality of Life and Fertility Performance in Endometriosis). Doctoral (PhD) Thesis, University of Pécs, Pécs, Hungary, **2024**.
5. Donnez, J.; Cacciottola, L.; Squifflet, J.-L.; Dolmans, M.-M. Profile of Linzagolix in the Management of Endometriosis, Including Design, Development and Potential Place in Therapy: A Narrative Review. *Drug Des. Dev. Ther.* **2023**, *17*, 369–380. DOI: 10.2147/DDDT.S269976
6. Fuqua, J.S.; Eugster, E.A. History of Puberty: Normal and Precocious. *Horm. Res. Paediatr.* **2022**, *95*, 568–578. DOI: 10.1159/000525386

7. Gonçalves, M.D.; Tomiotto-Pellissier, F.; De Matos, R.L.N.; Assolini, J.P.; Da Silva Bortoleti, B.T.; Concato, V.M.; Silva, T.F.; Rafael, J.A.; Pavanelli, W.R.; Conchon-Costa, I.; et al. Recent Advances in Biotransformation by *Cunninghamella* Species. *Curr. Drug Metab.* **2021**, *22*, 1035–1064. DOI: 10.2174/1389200222666211126100023

8. Al-Badr, A.A. Chapter Five – Danazol. In *Profiles of Drug Substances, Excipients and Related Methodology*; Al-Majed, A.A., Ed.; Academic Press: Cambridge, MA, USA, **2022**; Volume 47, pp. 149–326. DOI: 10.1016/bs.podrm.2021.10.005

9. Huang, H.-E.; Lin, K.-M.; Lin, J.-C.; Lin, Y.-T.; He, H.-R.; Wang, Y.-W.; Yu, S.-F.; Chen, J.-F.; Cheng, T.-T. Danazol in Refractory Autoimmune Hemolytic Anemia or Immune Thrombocytopenia: A Case Series Report and Literature Review. *Pharmaceuticals* **2022**, *15*, Art. No: 1377. DOI: 10.3390/ph15111377

10. Riva, M.; Bosi, A.; Rizzo, L.; Mazzon, F.; Ferrari, S.; Lussana, F.; Borin, L.; Castelli, A.; Cairoli, R.; Barcellini, W.; et al. Danazol Treatment for Thrombocytopenia in Myelodysplastic Syndromes: Can an "Old-Fashioned" Drug Be Effective? *HemaSphere* **2023**, *7*, Art. No: e867. DOI: 10.1097/HS9.0000000000000867

11. Nyamba, I.; Sombié, C.B.; Yabré, M.; Zimé-Diawara, H.; Yaméogo, J.; Ouédraogo, S.; Lechanteur, A.; Semdé, R.; Evrard, B. Pharmaceutical Approaches for Enhancing Solubility and Oral Bioavailability of Poorly Soluble Drugs. *Eur. J. Pharm. Biopharm.* **2024**, *204*, Art. No: 114513. DOI: 10.1016/j.ejpb.2024.114513

12. Madhuri, G.; Nagaraju, R. An Overview on Novel Particle Engineering Designing: Co-Crystallization Techniques. *Int. J. Pharm. Sci. Rev. Res.* **2021**, *66*, 88–101. DOI: 10.47583/ijpsrr.2021.v66i01.015

13. Jadhav, S.P.; Chaudhari, K.R.; Nikam, K.R.; Salunkhe, K.S.; Chaudhari, S.R. Co-Crystal: An Emerging Trend in Pharmaceuticals. *Inventi Rapid: NDDS* **2012**, *2012*(*3*), 1–6.

14. Dhondale, M.R.; Thakor, P.; Nambiar, A.G.; Singh, M.; Agrawal, A.K.; Shastri, N.R.; Kumar, D. Co-Crystallization Approach to Enhance the Stability of Moisture-Sensitive Drugs. *Pharmaceutics* **2023**, *15*, Art. No: 189. DOI: 10.3390/pharmaceutics15010189

15. Bhatia, M.; Kumar, A.; Verma, V.; Devi, S. Development of Ketoprofen-p-Aminobenzoic Acid Co-Crystal: Formulation, Characterization, Optimization, and Evaluation. *Med. Chem. Res.* **2021**, *30*, 2090–2102. DOI: 10.1007/s00044-021-02794-7

16. Tatsumi, Y.; Shimoyama, Y.; Kazarian, S.G. Analysis of the Dissolution Behavior of Theophylline and Its Cocrystal Using ATR-FTIR Spectroscopic Imaging. *Mol. Pharm.* **2024**, *21*, 3233–3239. DOI: 10.1021/acs.molpharmaceut.4c00002

17. Zhang, H.; Zeng, H.; Li, M.; Song, Y.; Tian, S.; Xiong, J.; He, L.; Liu, Y.; Wu, X. Novel Ascorbic Acid Co-Crystal Formulations for Improved Stability. *Molecules* **2022**, *27*, Art. No: 7998. DOI: 10.3390/molecules27227998

18. Chettri, A.; Subba, A.; Singh, G.P.; Bag, P.P. Pharmaceutical Co-Crystals: A Green Way to Enhance Drug Stability and Solubility for Improved Therapeutic Efficacy. *J. Pharm. Pharmacol.* **2024**, *76*, 1–12. DOI: 10.1093/jpp/rgad097

19. Al-Nimry, S.S.; Khanfar, M.S. Enhancement of the Solubility of Asenapine Maleate Through the Preparation of Co-Crystals. *Curr. Drug Deliv.* **2022**, *19*, 788–800. DOI: 10.2174/1567201818666210805154345

20. Huang, Z.; Staufenbiel, S.; Bodmeier, R. Combination of Co-Crystal and Nanocrystal Techniques to Improve the Solubility and Dissolution Rate of Poorly Soluble Drugs. *Pharm. Res.* **2022**, *39*, 949–961. DOI: 10.1007/s11095-022-03243-9

21. Ji, X.; Wu, D.; Li, C.; Li, J.; Sun, Q.; Chang, D.; Yin, Q.; Zhou, L.; Xie, C.; Gong, J.; et al. Enhanced Solubility, Dissolution, and Permeability of Abacavir by Salt and Cocrystal Formation. *Cryst. Growth Des.* **2022**, *22*, 428–440. DOI: 10.1021/acs.cgd.1c01051

22. Nadh, T.V.H.H.; Kumar, P.S.; Ramana, M.V.; Rao, N.R. Formulation and Optimization of Zolmitriptan Orodispersible Tablets. *J. Drug Deliv. Ther.* **2021**, *11*, 50–58. DOI: 10.22270/jddt.v11i3.4703

23. Kumar, S.; Sharma, P. Factorial Design Optimization in Pharmaceutical Formulations. *Asian J. Res. Chem.* **2021**, *14*, 245–252.

24. Jadhav, S.; Patil, M. Formulation of Tablet of Ivermectin Co-Crystal for Enhancement of Solubility and Other Physical Properties. *Res. J. Pharm. Technol.* **2023**, *16*, 1245–1252.

25. Abdelrahman, H.; Essa, E.; Maghraby, G.E.; Arafa, M. L-Proline as Co-Crystal Forming Amino Acid for Enhanced Dissolution Rate of Lamotrigine: Development of Buccal Tablet. *Indones. J. Pharm.* **2023**, *34*, 574–583. DOI: 10.22146/ijp.6867

26. Eidevåg, T.; Thomson, E.S.; Kallin, D.; Casselgren, J.; Rasmuson, A. Angle of Repose of Snow: An Experimental Study on Cohesive Properties. *Cold Reg. Sci. Technol.* **2022**, *194*, Art. No: 103470. DOI: 10.1016/j.coldregions.2021.103470

27. Singh, A.; Patel, R. Powder Flow Characterization in Pharmaceutical Manufacturing. *Res. J. Pharm. Technol.* **2021**, *14*, 156–162.

28. Al-Dulaimi, A.F.; Al-Kotaji, M.; Abachi, F.T. Paracetamol/Naproxen Co-Crystals: A Simple Way for Improvement of Flowability, Tableting and Dissolution Properties. *Iraqi J. Pharm. Sci.* **2021**, *30*, 45–55.

29. Botella-Martínez, C.; Viuda-Martos, M.; Fernández-López, J.A.; Pérez-Alvarez, J.A.; Fernández-López, J. Development of Plant-Based Burgers Using Gelled Emulsions as Fat Source and Beetroot Juice as Colorant. *LWT* **2022**, *172*, Art. No: 114193. DOI: 10.1016/j.lwt.2022.114193

30. Simão, J.; Chaudhary, S.A.; Ribeiro, A.J. Implementation of Quality by Design (QbD) for Development of Bilayer Tablets. *Eur. J. Pharm. Sci.* **2023**, *184*, Art. No: 106412. DOI: 10.1016/j.ejps.2023.106412

31. Ficzere, M.; Mészáros, L.A.; Kállai-Szabó, N.; Kovács, A.; Antal, I.; Nagy, Z.K.; Galata, D.L. Real-Time Coating Thickness Measurement and Defect Recognition of Film-Coated Tablets with Machine

Vision and Deep Learning. *Int. J. Pharm.* **2022**, *623*, Art. No: 121957. DOI: 10.1016/j.ijpharm.2022.121957

32. Momeni, M.; Afkanpour, M.; Rakhshani, S.; Mehrabian, A.; Tabesh, H. Prediction Model Based on Artificial Intelligence Techniques for Disintegration Time and Hardness of Fast Disintegrating Tablets. *BMC Med. Inform. Decis. Mak.* **2024**, *24*, Art. No: 88. DOI: 10.1186/s12911-024-02485-4
33. Zhao, H.; Yu, Y.; Ni, N.; Zhao, L.; Lin, X.; Wang, Y.; Du, R.; Shen, L. New Parameter for Characterization of Tablet Friability. *Int. J. Pharm.* **2022**, *611*, Art. No: 121339. DOI: 10.1016/j.ijpharm.2021.121339
34. Berardi, A.; Bisharat, L.; Quodbach, J.; Abdel Rahim, S.; Perinelli, D.R.; Cespi, M. Advancing the Understanding of Tablet Disintegration Phenomenon. *Int. J. Pharm.* **2021**, *598*, Art. No: 120390. DOI: 10.1016/j.ijpharm.2021.120390
35. Farquharson, A.; Gladding, Z.; Ritchie, G.; Shende, C.; Cosgrove, J.; Smith, W.; Brouillette, C.; Farquharson, S. Drug Content Uniformity Using Raman Spectroscopy. *Pharmaceutics* **2021**, *13*, Art. No: 309. DOI: 10.3390/pharmaceutics13030309
36. Chakraborty, S.; Mondal, D.S. Green Eco-Friendly Analytical Method Development of Favipiravir. *Int. J. Pharm. Investig.* **2023**, 13, 290–305. DOI: 10.5530/ijpi.13.2.039
37. González-González, O.; Ramirez, I.O.; Ramirez, B.I.; O'Connell, P.; Ballesteros, M.P.; Torrado, J.J.; Serrano, D.R. Drug Stability: ICH versus Accelerated Predictive Stability Studies. *Pharmaceutics* **2022**, *14*, Art. No: 2324. DOI: 10.3390/pharmaceutics14112324
38. Parvarinezhad, S.; Salehi, M.; Kubicki, M.; Eshaghi Malekshah, R. Noncovalent Interactions in Co-Crystal of μ-Oxobridged Polymeric Copper(II) Complex. *J. Mol. Struct.* **2022**, *1260*, Art. No: 132780. DOI: 10.1016/j.molstruc.2022.132780
39. Rojek, B.; Bartyzel, A.; Leyk, E.; Plenis, A. Arbidol Hydrochloride Compatibility Study Using DSC, FTIR, TGA-FTIR, and PXRD. *J. Therm. Anal. Calorim.* **2025**, *152*, 1–15. DOI: 10.1007/s10973-025-14056-4
40. Farag Badawy, S.I.; Ghorab, M.M.; Adeyeye, C.M. Characterization and Bioavailability of Danazol–Hydroxypropyl ß-Cyclodextrin Coprecipitates. *Int. J. Pharm.* **1996**, *128*, 45–54. DOI: 10.1016/0378-5173(95)04214-8
41. Bhalani, D.V.; Nutan, B.; Kumar, A.; Singh Chandel, A.K. Bioavailability Enhancement Techniques for Poorly Aqueous Soluble Drugs. *Biomedicines* **2022**, *10,* Art. No: 2055. DOI: 10.3390/biomedicines10092055
42. Han, J.; Li, L.; Su, M.; Heng, W.; Wei, Y.; Gao, Y.; Qian, S. Deaggregation and Crystallization Inhibition in Co-Amorphous Systems. *Pharmaceutics* **2021**, *13*, Art. No: 1725. DOI: 10.3390/pharmaceutics13101725
43. Adama, J.C.; Arocha, C.G.; Ogbobe, P.O. Physical Properties of Oil Palm Kernels. *Niger. J. Technol.* **2022**, *41*, 365–369. DOI: 10.4314/njt.v41i2.18
44. Kole, S.; Vinchurkar, R.; Gawade, A.; Kuchekar, A. Impact of Co-Crystal Formation on Stability of Camylofin Tablets. *Hacet. Univ. J. Fac. Pharm.* **2024**, *44*, 108–123. DOI: 10.52794/hujpharm.1331991
45. Lovanov, R.; Cornilă, A.; Bogdan, C.; Hales, D.; Tomuță, I.; Achim, M.; Tăut, A.; Iman, N.; Casian, T.; Iurian, S. Disintegration and Texture-Related Palatability of Orodispersible Tablets. *Eur. J. Pharm. Sci.* **2024**, *198*, Art. No: 106801. DOI: 10.1016/j.ejps.2024.106801
46. Devi, S.; Kumar, A.; Kapoor, A.; Verma, V.; Yadav, S.; Bhatia, M. Ketoprofen–FA Co-Crystal: In Vitro and In Vivo Investigation. *AAPS PharmSciTech* **2022**, *23*, Art. No: 101. DOI: 10.1208/s12249-022-02253-5
47. Zarrik, B.; El Amri, A.; Bensalah, J.; Jebli, A.; Lebkiri, A.; Hsissou, R.; Hbaiz, E.M.; Rifi, E.H.; Lebkiri, A. Adsorption of Crystal Violet Using Graphene Oxide Composite. *Inorg. Chem. Commun.* **2024**, *162*, Art. No: 112179. DOI: 10.1016/j.inoche.2024.112179
48. Mazloomi, S.; Amarloei, A.; Gholami, F.; Haghighat, G.A.; Badalians Gholikandi, G.; Nourmoradi, H.; Mohammadi, A.A.; Fattahi, M.; Nguyen Le, B. Process Modeling for Metronidazole Removal by ZIF-67 Crystals. *Sci. Rep.* **2023**, *13*, Art. No: 14654. DOI: 10.1038/s41598-023-41724-y
49. Ruhil, S.; Dahiya, M.; Kaur, H.; Singh, J. Disintegration Profiling of Rapidly Disintegrating Tablets by Thermal Imaging. *Int. J. Pharm.* **2022**, *611*, Art. No: 121283. DOI: 10.1016/j.ijpharm.2021.121283
50. Hu, C.; Zhang, F.; Fan, H. Evaluation of Drug Dissolution in Co-Amorphous and Co-Crystal Systems. *AAPS PharmSciTech* **2021**, *22*, Art. No: 21. DOI: 10.1208/s12249-020-01864-0
51. Janilkarn-Urena, I.; Tse, A.; Lin, J.; Tafolla-Aguirre, B.; Idrissova, A.; Zhang, M.; Skinner, S.G.; Mostowfi, N.; Kim, J.; Kalapatapu, N.; et al. Improving Solubility of Pseudo-Hydrophobic Chemicals through Co-Crystal Formulation. *PNAS Nexus* **2025**, *4*, Art. No: pgaf007. DOI: 10.1093/pnasnexus/pgaf007
52. Orszulak, L.; Włodarczyk, P.; Hachuła, B.; Lamrani, T.; Jurkiewicz, K.; Tarnacka, M.; Hreczka, M.; Kamiński, K.; Kamińska, E. Inhibition of Naproxen Crystallization by Polymers. *Eur. J. Pharm. Biopharm.* **2025**, *207*, Art. No: 114581. DOI: 10.1016/j.ejpb.2024.114581
53. Jadhav, S.P.; Ahire, S.M.; Shewale, V.V.; Patil, C.D.; Pagar, R.Y.; Sonawane, D.D.; et al. Formulation of Tablet of Nifedipine Co-Crystal for Enhancement of Solubility. *Biosci. Biotechnol. Res. Asia* **2025**, *22(1),* 191–200. DOI: 10.13005/bbra/3353